



Article citation info:

Du S, Yang Y., Study on the influence of pin shaft clearance on the bearing performance of the hydraulic support, *Eksploracja i Niezawodność – Maintenance and Reliability* 2023; 25(4) <http://doi.org/10.17531/ein/174367>

Study on the influence of pin shaft clearance on the bearing performance of the hydraulic support

Indexed by:



Shunyi Du^a, Yang Yang^{a,*}

^a Shandong University of science and technology, China

Highlights

- This study addresses the often-neglected issue of pin clearance by developing a dynamic simulation model for hydraulic support using the Lankarani-Nikravesh (L-N) contact model. Hydraulic support behavior with pin clearance is analyzed through the simulation.
- A comparative assessment of bearing capacity of hydraulic support is conducted with and without clearance, highlighting the effects of clearance size and position on bearing capacity.
- An orthogonal test group is designed to explore bearing capacity of hydraulic support variation in multi-clearance coupling scenarios, underscoring the importance of investigating pin clearance.

Abstract

The pin clearance is a significant factor affecting the bearing capacity of the hydraulic support, but the effect of the pin clearance is often neglected in the current studies. Therefore, on the basis of considering the Equal stiffness spring damping system of the column, the dynamic simulation model of the hydraulic support without clearance was constructed to study the static bearing capacity of the hydraulic support. Moreover, as per the contact model of the connecting pin clearance, the dynamic simulation model of the single-pin clearance hydraulic support was established. The effect of single pin clearance on the load of the front and rear columns of the hydraulic support and the transmission force at key bearing points was analyzed. Meanwhile, the influence of single pin clearance at different positions on the bearing capacity of the hydraulic support was compared. Through the design of orthogonal test, the change of the transmission force of the bearing points under the coupling of multi-pin clearance was studied.

Keywords

bearing capacity, orthogonal test, hydraulic support, pin clearance, multi-clearance coupling.

This is an open access article under the CC BY license (<https://creativecommons.org/licenses/by/4.0/>)

1. Introduction

Hydraulic support is one of the most crucial supporting devices in coal mine, its safe and efficient bearing capacity is extremely important to the security of coal mining and the personal safety of mine operators [27,31]. However, with the increase in the demand for coal mining, support and transportation adaptive collaborative construction of unmanned intelligent mining face, as well as deep coal mining and complex geological conditions, higher requirements are put forward for the bearing performance and bearing safety of hydraulic supports, which require better bearing performance and bearing reliability of hydraulic supports [17,25,26]. Therefore, it is very necessary to

study the bearing performance of the hydraulic support, and it is of great significance to design and optimize the hydraulic support with better bearing performance and higher applicability.

For the sake of optimizing and improving the bearing capacity of hydraulic support, a great deal of research has been done on the structure and working characteristics of the hydraulic support by many scholars. Meng [16] et al. studied the coupling response of the support under impact load through the machine-liquid coupling co-simulation technology, and pointed out that the front column is more sensitive to the impact load

(*) Corresponding author.

E-mail addresses:

S. Du, sdkdshunyiidu@126.com, Y. Yang (ORCID: 0000-0001-6304-6362) yang.yang@sdust.edu.cn

and may reduce the hinge position of the support. Ren [20], Zeng [33], Bu [5] et al studied the response of various components of hydraulic support under dynamic load. Wang [28] and Wan [22] have done a great deal of study on the control of the surrounding rock and the stability of the hydraulic support, and gave important factors affecting the stability of large mining height hydraulic support. Cao et al. [6] studied the dynamic loading performance of hydraulic support under variable loading conditions and optimized the top beam structure. Wan [23] et al. analyzed the performance of the new equilibrium jack under the pressure bumping and concluded that the new equilibrium jack has better impact resistance. Wang [30] et al. investigated the stress response and working characteristics of the hydraulic support column. Hu et al. [12] indicated that the higher the acceleration of the hydraulic support lifting frame, the higher the impact on the force of each hinged joint and the bearing capacity of the support. Ge et al. [9] pointed out a method for adjusting the position of a hydraulic support group in the working face. Pang et al. [18] investigated the solution method of hydraulic support attitude and support height by using the stroke of jack. Zhang [35], Zeng [34], Wang [24] et al. proposed a variety of feasible monitoring methods for the attitude of hydraulic support group. Tian et al. [21] proposed a six-column backfill hydraulic support for supporting the roof of the working surface. Guan [10] et al. designed a double parallelogram structure hydraulic support and analyzed the working characteristics of the balancing jack and the column. Li [15] et al. studied and compared the load-bearing capacity of four-column and two-column caving hydraulic supports.

To sum up, the current research on the bearing performance of hydraulic support is usually based on the premise of ignoring the connection pin shaft or not considering the pin clearance. For example, when using ADAMS and other software to study the dynamic characteristics of hydraulic support, in order to facilitate the establishment of simulation models or simplify the research, the pin connection unit is often equivalent to a rotating pair between two parts connected through the pin, and the influence of the assembly clearance between the pin and the ear seat on the performance of the hydraulic support is ignored.

However, the clearance between the pin will cause a nonlinear dynamic response between the heavy-load mechanical connectors. The nonlinear contact behavior will

cause a large contact force between the pin and the inner wall of the ear seat under the condition of a very small clearance, inducing contact deformation, and even irreversible deformation or damage in serious cases. As shown in Figure 1, in the actual working process, the hydraulic support will produce plastic deformation, leading to an increase in the clearance size of the pin. In severe cases, this deformation can even result in the fracture of the pin and the cracking of the ear seat, causing a failure in the support function of the hydraulic support. Moreover, it can pose significant safety risks when subjected to overload, wear, and rust. At the same time, the existence of pin connection clearance will change the transmission relationship between different components, thus increasing the movement instability during the lifting frame of hydraulic support, and affecting the attitude change of key bearing components such as the top beam, which will threaten the dynamic performance and support state of the support to a certain extent [29,32].



Fig. 1. pin connection of hydraulic support.

Therefore, in an effort to study the effect of pin clearance on the bearing capacity of hydraulic support. Firstly, the column is equivalent to the Equal stiffness spring damping system, and the dynamic simulation model of the hydraulic support without clearance is constructed by ADAMS, which studies the static bearing capacity of the hydraulic support without clearance. Secondly, as per the Lankarani-Nikravesh (L-N) contact model [14] and the improved Coulomb friction model [1,2], a dynamic simulation model of single-pin clearance hydraulic support was built to analyze variation of the load on the front and rear columns and the transmission force at each bearing point under

single-pin clearance size. The effect of single pin clearance position change on the bearing capacity of the hydraulic support was also studied. Finally, through the design of orthogonal experimental group, the change of the transmission force of each bearing point of under the coupling condition of multi-pin clearance is studied.

2. Static load bearing capacity of non-clearance hydraulic support

2.1. Construction of Equal stiffness spring damping system of column

Under normal circumstances, the hydraulic support be influenced by the complex load such as roof pressure and periodic pressure, which will cause the working load and the supporting height of the column to constantly change dynamically. Therefore, for the purpose of better simulate the dynamic changes of the column under the influence of external loads, the method of replacing the column with an equal-stiffness spring damping system is used, as shown in Figure 2.

The equivalent stiffness K_C of the column can be calculated

by the following as:

$$K_c = \frac{\pi D^2 E}{L} \quad (1)$$

where, K_c is the equivalent stiffness, N/m; E is bulk modulus of elasticity, Pa, choose 1.95×10^9 Pa; D is the bearing cavity diameter, m ; L is the liquid column length, m .

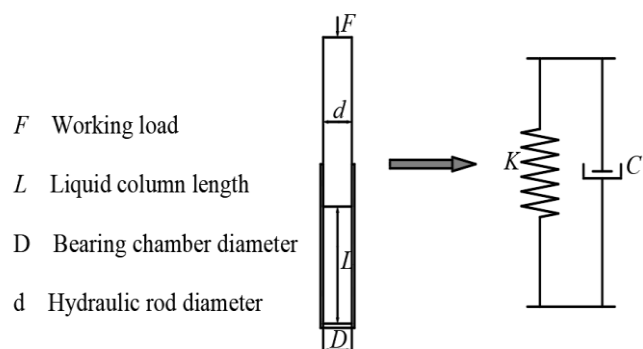


Fig. 2. Column equal stiffness spring damping system.

According to the data in Table 1 and combined with formula 1, it can be calculated that the equivalent stiffness of the front column is 9.69×10^7 N/m, and that of the rear column is 9.76×10^7 N/m.

Table. 1. parameters of front and rear column.

Columns	Bearing chamber diameter/mm	Hydraulic rod diameter/mm	Liquid column length/mm
front columns	230	210	836
rear column	230	210	830

2.2. Construction of dynamic simulation model of non-clearance hydraulic support

Figure 3 displays the model for dynamically simulating the hydraulic support.

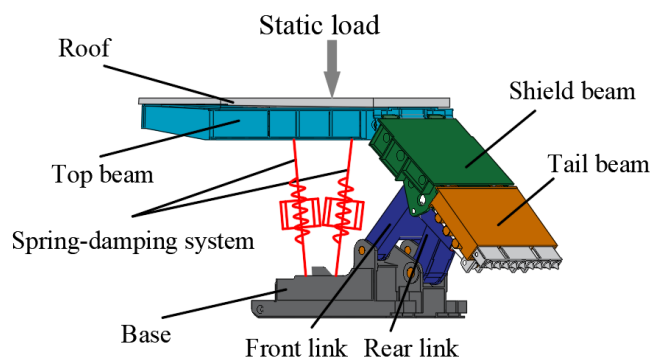


Fig. 3. Dynamic simulation model of non-clearance hydraulic support.

The base is connected to the ground by a fixed pair, the roof is

constrained to the top beam by a collision contact, either the shield beam and the top beam, or the front and rear link and the shield beam or base, or the shield beam and the tail beam are connected by a rotating pair. Moreover, the column is substituted by an equal stiffness spring damping system.

The roof material is defined as coal, the pin material as 35CrMo, and the other parts of the support as steel. The main properties of the materials are displayed in Table 2.

Table. 2. Main properties of materials.

materials	Density ($\text{kg} \times \text{mm}^{-3}$)	Poisson ratio	Elastic modulus (MPa)
coal	1.3×10^{-6}	0.28	2.2×10^3
steel	7.801×10^{-6}	0.29	2.07×10^5
35CrMo	7.850×10^{-6}	0.3	2.06×10^5

2.3. Static bearing capacity analysis of non-clearance hydraulic support

As per the performance argument of the hydraulic support studied in this article, the pressure of the roof is 5000KN to

simulate the static load status to the hydraulic support. The specific load is symmetrically applied to the roof by STEP (time,0,0,1,2500000) on both sides. The position of the load is displayed in Figure 3(the loading position is 1100mm from the end of the top beam and is on the column socket connection line of the front and rear columns), and the duration of the entire simulation process is 1.5s. The transmission force response of the load on the front and rear columns and each bearing point under stable state is obtained. The rear link - base connection point is named as bearing point 1, the front link - base connection point is bearing point 2, the rear link - shield beam connection point is bearing point 3, the front link - shield beam connection point is bearing point 4, and the connection point of top team-shield beam is bearing point 5. Figure 4 shows the dynamic characteristics curve of the column under static load of the hydraulic support.

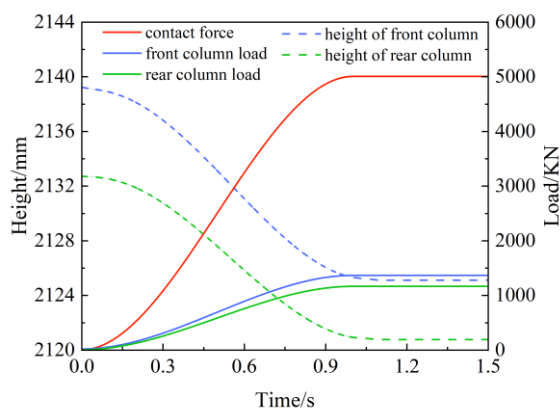


Fig. 4. static load response of Column.

It is observed from the figure 4 that when the system is stable, the contact force between the roof and the top beam is stable at 5006kN, which is basically consistent with the applied roof pressure. The load borne by the front and rear columns is 1368kN and 1166kN respectively. The compression of the equivalent spring damping system of the front and rear columns is 14.12mm and 11.95mm, respectively. It can be concluded that the spring-damping system stiffness value of the front and rear columns has little difference with the theoretical calculation value.

Table 3 displays the transmission force of each bearing point. It can be discerned that the working condition at bearing point 1 and bearing point 3 is the worst, which has a tremendous influence on the bearing capacity of the hydraulic support.

Table. 3. Transmission force of bearing point without clearance.

Location	Point 1	Point 2	Point 3	Point 4	Point 5
Connection location	rear link - base	front link - base	rear link - shield beam	front link - shield beam	top team-shield beam
Transmission force	391.3kN	256.4kN	395.7kN	253.9kN	83.9kN

3. Bearing capacity of hydraulic support with single pin clearance

3.1. Establishment of pin clearance contact theoretical model

As shown in Figure 5, at the point where each component of the hydraulic support is connected to the pin, there will inevitably be a certain matching clearance between the pin and the ear seat.

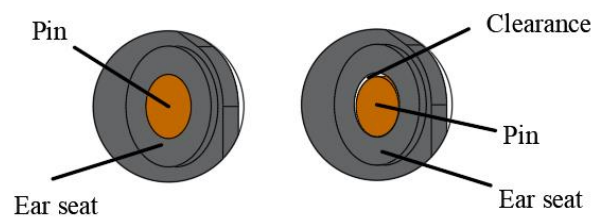


Fig. 5. Comparison of pin connection.

Therefore, in an effort to better display the clearance state and contact characteristics of the connection pin fit, the collision and articulation model shown in Figure 6 is adopted to simulate the connection relationship between the connected parts [19].

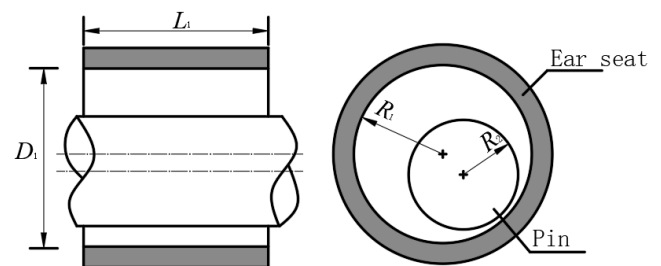


Fig. 6. Collision articulation model.

In the collision articulation model, the pin and the ear seat at the joint are regarded as two elastic colliders, and the rotational motion constraint between the pin and the ear seat is replaced by the collision contact force constraint.

Assuming that the internal surface of the ear seat and the external surface of the pin are regular circles, the clearance value between the pin and the ear seat can be defined as:

$$c = \Delta R = R_1 - R_2 \quad (2)$$

where, R_1 and R_2 respectively represent the radius values of the ear seat and the pin.

Figure 7 displays the mathematical model of pin clearance

established based on the collision and articular model in Figure 6 [8], where O_1 is the central point of the internal surface of the ear seat and O_2 is the central point of the external surface of the pin shaft. r_1 and r_2 are the position vectors of the ear seat and the pin in XOY coordinate system, then the joint clearance vector of the ear seat and the pin is:

$$c_{12} = r_1 - r_2 \quad (3)$$

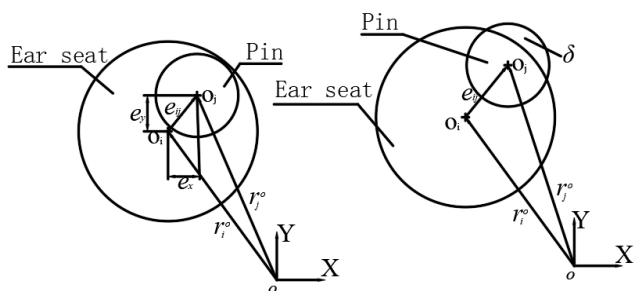


Fig.7. Mathematical model of pin clearance.

When contact collision occurs between ear seat and pin, the contact penetration deformation inflicted by contact collision can be expressed as:

$$\delta = c_{12} - c \quad (4)$$

Therefore, the size is used to determine whether there is a contact collision between the pin and the ear seat, and the judging method is as follows:

$$\begin{cases} \delta < 0 & \text{No contact, free movement} \\ \delta = 0 & \text{Initiate contact or disengage} \\ \delta > 0 & \text{Contact, elastic deformation} \end{cases} \quad (5)$$

3.2. Contact collision force model

As demonstrated in Figure 8, the interaction collision force will emerge, when contact collision occurs between ear seat and pin. In addition, the contact collision force can be decomposed into the normal contact force F_n generated by elastic deformation of the material and the tangential contact force F_t generated by the relative movement of the ear seat and the pin seat.

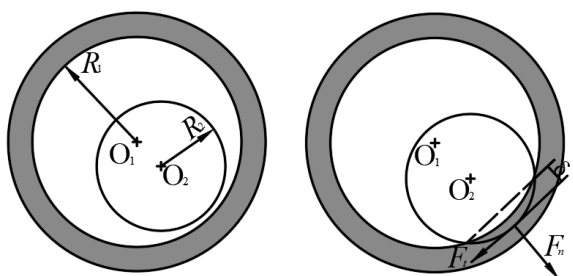


Fig. 8. Pin contact collision.

The nonlinear spring damping collision contact force model is presented in accordance with L-N, and the normal contact force formula of this model is [4,13,14,]:

$$F_n = K\delta^n + D\dot{\delta} \quad (6)$$

where, K is the contact stiffness; δ is the penetration deformation; D is the damper coefficient; $\dot{\delta}$ is the relative velocity during the collision.

The expression of equivalent contact stiffness is as follows [3,11]:

$$K = \frac{4\sqrt{R}}{3\pi(\sigma_1 + \sigma_2)} \quad (7)$$

$$\sigma_i = \frac{1 - \nu_i^2}{\pi E_i}, \quad (i = 1, 2) \quad (8)$$

$$R = \frac{R_1 R_2}{R_1 \pm R_2} \quad (9)$$

where, σ_i is the material coefficients of contact object; ν_i is Poisson's ratio; E_i is the elastic modulus; R is the equivalent radius, where a plus sign is used for external contact and a minus sign is used for internal contact.

As shown in Figure 9, as per the improved Coulomb law [7] in ADAMS software, tangential friction force of internal contact can be definite as:

$$F_T = \mu_{(V_t)} F_N \quad (10)$$

where, F_N is the normal contact force; $\mu_{(V_t)}$ is the dynamic friction coefficient, and its function expression is as follows:

$$\mu(V_t) = \begin{cases} -\text{sign}(V_t) \cdot \mu_d & |V_t| > V_d \\ -\text{step}(|V_t|, V_d, \mu_d, V_s, V_s) \cdot \text{sign}(V_t) & V_s \leq |V_t| \leq V_d \\ \text{step}(V_t, -V_s, \mu_s, V_s, -\mu_s) & |V_t| < V_d \end{cases} \quad (11)$$

where, V_T is the relative motion speed; V_s And V_d are specific speed limits; μ_s and μ_d are static friction coefficient and dynamic friction coefficient respectively.

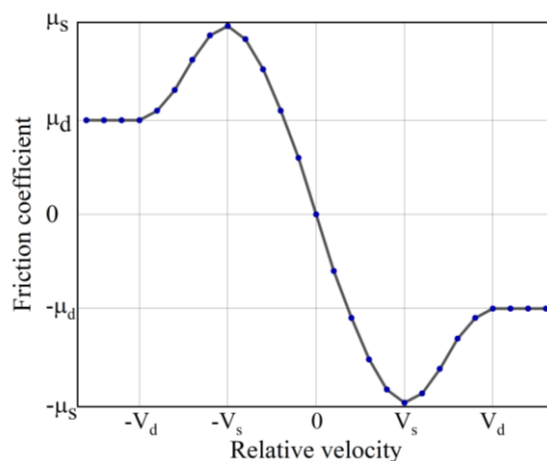


Fig. 9. Coulomb friction curve.

3.3. Construction of dynamic simulation model of single-pin clearance hydraulic support

On the basis of the dynamic simulation model of the non-clearance hydraulic support, the rotating pair connection at the pin 1 is replaced by the pin clearance contact model, so as to build the dynamic simulation model of the single-pin clearance hydraulic support, where the contact stiffness K is calculated by equation (7-9) and Table (2,4). In order to distinguish the single pin in different positions, the pin at the base - rear link and the base - front link are defined as pin 1 and 2, the pin at the shield beam-rear link and the shield beam-front link are pin 3 and pin 4, and the pin at the top beam-shield beam are pins 5. The initial radius of each pin is shown in Table 4. The constraint conditions and static load forms between other components are consistent with those in the non-clearance hydraulic support.

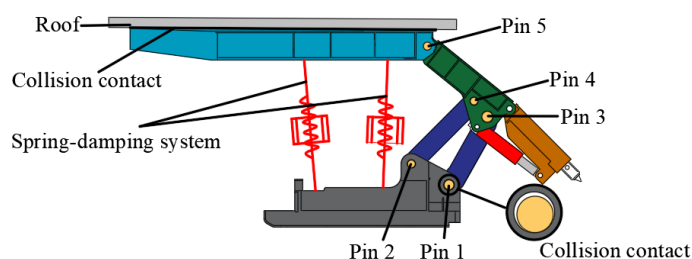


Fig. 10. Dynamic simulation model of single pin clearance hydraulic support.

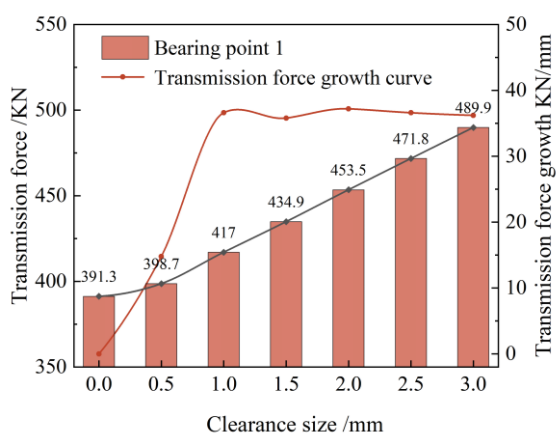
Table. 4. Initial pin radius.

Pin position	Pin 1	Pin 2	Pin 3	Pin 4	Pin 5
Radius	65.5mm	50.5mm	70mm	50.5mm	50.5mm

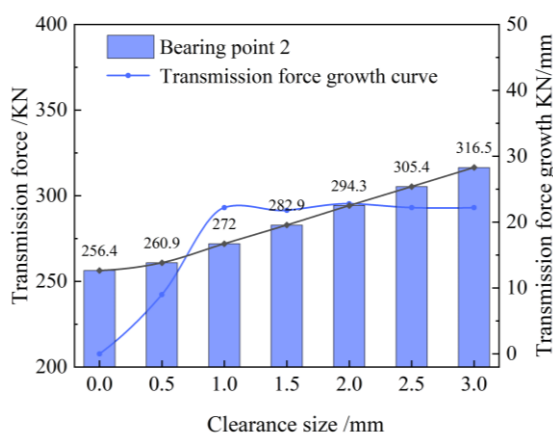
3.4. The influence of single clearance size on the bearing capacity of hydraulic support

In the actual work of the hydraulic support, the maximum clearance of the pin should generally be less than 1.5mm. In an effort to analyze the impact of the single pin clearance size on the bearing capacity of the hydraulic support, the pin clearance is set within the range of 0-3mm, in which the single clearance increment is 0.5mm. As per the simulation model of single-pin clearance hydraulic support built in 3.3, the static load simulation analysis is carried out on the different clearance size of the pin 1, and the transmission force response of the front and rear columns and each bearing point under stable state is obtained. Among them, the transmission force refers to the hinge force between the two parts of the support when there is no clearance, when there is a clearance, refers to the contact force of the clearance contact model.

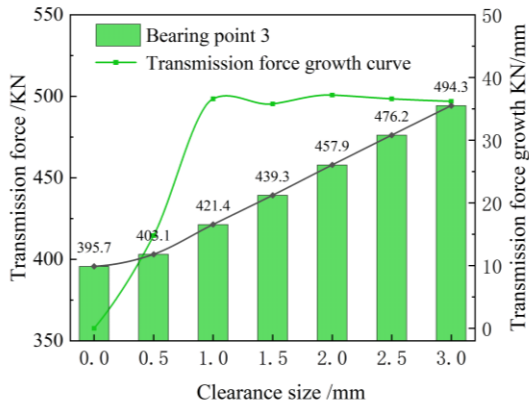
Figure 11 shows the influence of the single clearance size on the transmission force of the bearing point. First of all, it can be observed from the change of transmission force of each bearing point without clearance and with clearance that when there is a single clearance, the transmission force of each bearing point is significantly greater than that without clearance. When the single clearance size is 0.5mm, the transmission force increase ratio of bearing point 1-5 is 1.89%, 1.76%, 1.87%, 1.74%, 1.49%, respectively, indicating that a single clearance may lead to the increase of transmission force of the bearing point, and thus the working condition of each bearing point becomes worse under the same load.



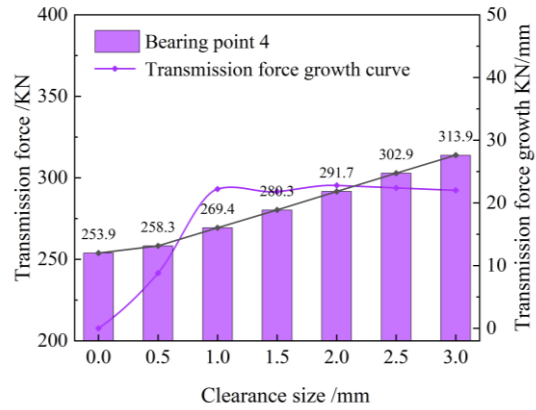
(a) Bearing point 1 transmission force



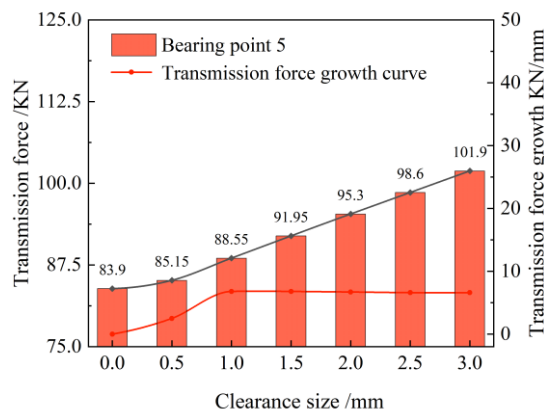
(b) Bearing point 2 transmission force



(c) Bearing point 3 transmission force



(d) Bearing point 4 Transmission force



(e) Bearing point 5 transmission force

Fig. 11. Transmission force response of the bearing point with a single clearance size.

Moreover, under different single clearance size, the transmission force of each bearing point is also different. In Figure (a), when the clearance is 1mm, the transmission force of bearing point 1 is 417KN, when the clearance is 2mm, it is 453.5KN, and when the clearance is 3mm, it is 489.9KN, compared with no clearance, the transmission force increases were 6.57%, 15.90% and 25.20%, respectively. Meanwhile, the change trend of the transmission force of other bearing points in Figure (b-e) is similar to that of bearing point 1. Obviously, increasing the size of a single clearance will lead to an increase in the transmission force of the bearing point

In addition, taking bearing point 1 as an example, for each change of 0.5mm clearance value, the corresponding change of transmission force is 7.4KN, 18.3KN, 17.9KN, 18.6KN, 18.3KN, 18.1KN. Combined with the transmission force growth curve of each bearing point in Figure 11, it can be found that the transmission force growth rate of the bearing point is slow, when the clearance size is within the range of 0-0.5mm. However, when the clearance size is greater than 0.5mm,

transmission force growth rate of the bearing point is accelerated, and when the clearance size is more than 1mm, the transmission force growth rate of the bearing point is basically stable.

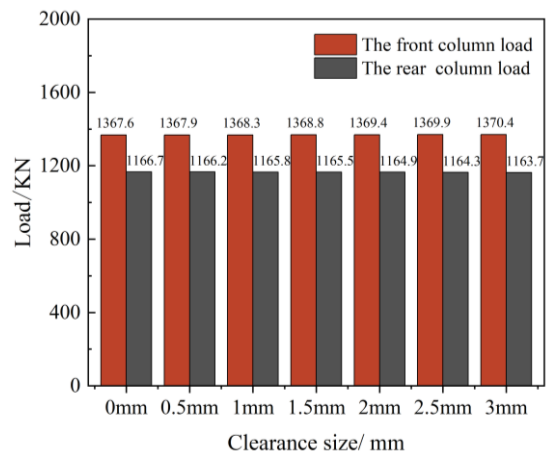


Fig. 12. Load response of front and rear columns with a single clearance size.

Figure 12 shows the load changes of the front and rear columns with a single clearance. As can be seen from the load value marked in the figure,, in comparison to the scenario

without clearance, the load of the front column increases slightly when there is a clearance, while the load of the rear column decreases slightly. However, the load of the front and rear columns changes little with the change of the clearance size.

Therefore, under the same bearing conditions, the single pin clearance may cause to the rise of the transmission force at the bearing point, with the gradual increase of the clearance size, the growth rate of the transmission force changes from slow to fast and then to stable law. When the clearance size is 3mm, the value increment of the transmission force at the bearing point 1-5 is the most serious, with an increase rate of 25.20%, 23.44%, 24.92%, 23.63% and 21.45%, respectively. Thus, reducing the bearing capacity of the hydraulic support. Furthermore, the larger the clearance size, the more pronounced the effect on the hydraulic support's bearing capacity.

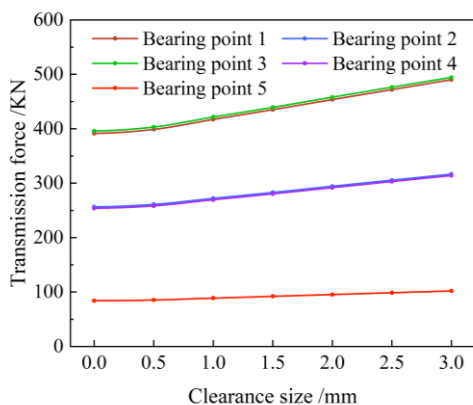
3.5. Influence of single clearance position on bearing capacity of hydraulic support

In the previous section, the bearing capacity of the hydraulic support was examined in relation to variations in the size of the single pin clearance. For the purpose of comparing the effect of varying single pin clearance positions on the bearing capacity of the hydraulic support, four different clearance positions including pin 1-4 were selected for simulation analysis.

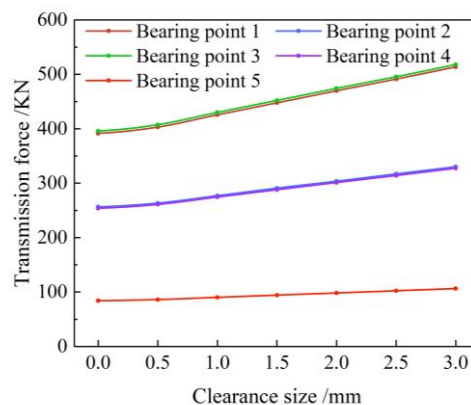
Figure 13 shows the variation trend of transmission force at

each bearing point under different single clearance positions. As evident from the figure, the single clearance at different positions all cause to the rise of the transmission force at each bearing point, and the transmission force at the bearing point shows an obvious growth trend with the rise of the clearance size. However, under the single clearance at different positions, the transmission force at each bearing point shows a basically consistent change trend with the clearance size.

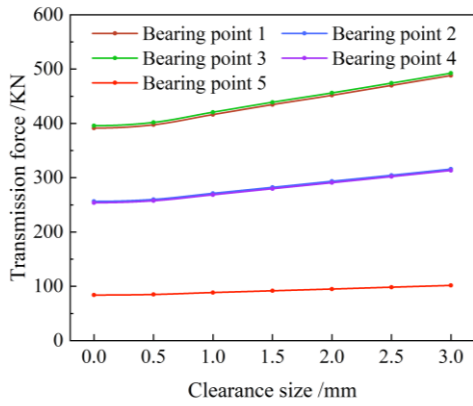
In addition, by comparing the transmission force of each bearing point under a single clearance at different positions, it can be seen that the transmission force of bearing point 3 and bearing point 1 is the largest, that of bearing point 2 and bearing point 4 is the second, and the transmission force of bearing point 5 is the least. When the single clearance size is 3mm, the multiplication factor of the force transmitted at the bearing point 3 and the bearing point 1 (the two ends of the rear connecting rod are connected to the pin) is about 1.5 compared with the bearing point 2 and the bearing point 4 (the two ends of the front connecting rod are connected to the pin), and is about 4.8 compared with the bearing point 5 (the top-shield beam is connected to the pin). Therefore, the working conditions at bearing point 3 and bearing point 3 are relatively worst, which exerts the most significant influence on the hydraulic support's bearing capacity and should be a focal point during the design process.



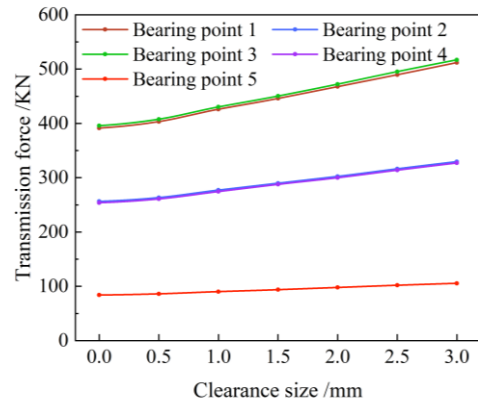
(a) Clearance position 1



(b) Clearance position 2



(c) Clearance position 3

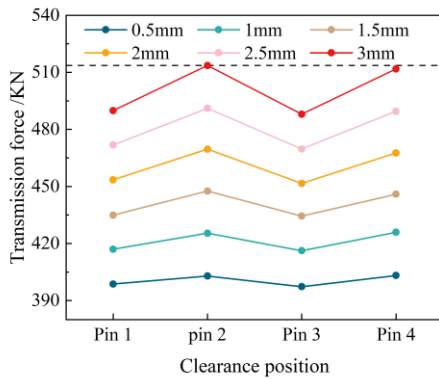


(d) Clearance position 4

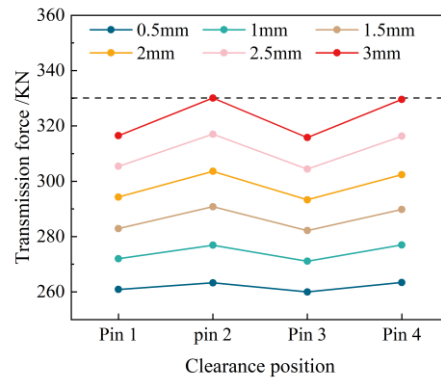
Fig. 13. Variation trend of transmission force at different clearance positions.

Figure 14 illustrates how different clearance positions impact the transmission force at the same bearing point. By observing the figure 12(a), it can be intuitively seen that under the same clearance, the clearance at the position of pin 2 and pin 4 has a considerable effect on the transmission force at the bearing point 1, while the clearance at the position of pin 1 and pin 3 has a lesser influence. As can be seen from the comparison

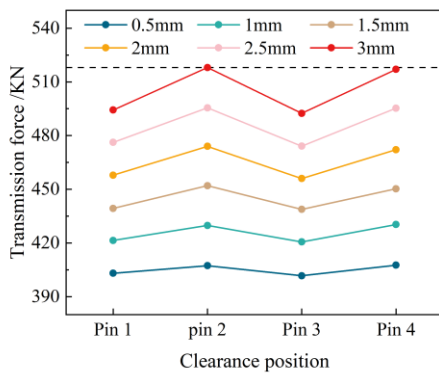
figure (a-e), the clearance at pin 2 has the most significant influence on the transmission force at each bearing point, while the clearance at pin 3 has the least influence on the transmission force at each bearing point. In addition, the greater the clearance between the pin and ear seat, the larger the clearance size, the more obvious the difference in sensitivity of different clearance positions to the transmission force of the bearing point.



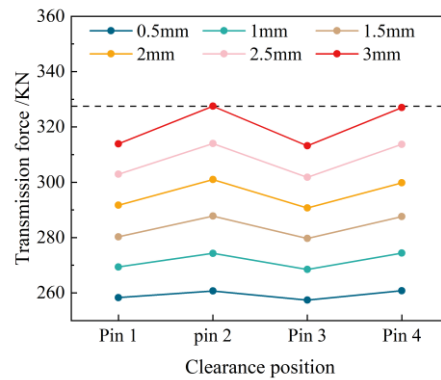
(a) Bearing point 1 transmission force



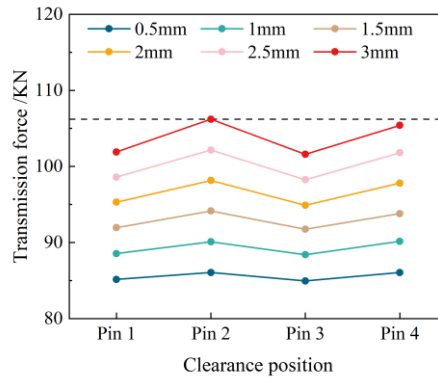
(b) Bearing point 2 transmission force



(c) Bearing point 3 transmission force



(d) Bearing point 4 transmission force



(e) Bearing point 5 transmission force

Fig. 14. effect of different clearance positions on the transmission force of bearing point.

Table 5 shows the load changes of front and rear columns under varying single clearance positions. It can be seen that when the single clearance position is pin 2, pin 3, pin 4, the load of front and rear columns is basically unchanged. Combined

with the data in figure 12, it can be concluded that the connecting pin clearance at both ends of the front and rear links have little impact on the load of the front and rear columns.

Table. 5. Load response of front and rear columns at different clearance positions.

Clearance size	Front column load /kN			Rear column load /kN		
	Pin 2	Pin 3	Pin 4	Pin 2	Pin 3	Pin 4
0.5mm	1367.9	1367.8	1367.8	1166.3	1166.2	1166.5
1mm	1368.4	1368.1	1368.3	1165.9	1166.5	1166.3
1.5mm	1369	1368.6	1368.8	1165.5	1165.9	1165.7
2mm	1369.6	1369.4	1369.4	1165.1	1164.7	1165.2
2.5mm	1370.1	1369.9	1370.1	1164.9	1164	1165
3mm	1370.8	1370.6	1370.3	1164.3	1163.2	1164.4

4. Multi-clearance coupling on the bearing capacity of hydraulic support

4.1. Multi-clearance coupling mode determination based on orthogonal text

In the previous chapter, the bearing capacity of hydraulic support is analyzed in relation to variations in the size of a single clearance, through establishment of the dynamic model for the a single-pin clearance support. In order to study the effect of multi-clearance coupling on the bearing capacity of the hydraulic support, based on dynamic simulation model of the single-pin clearance hydraulic support, as shown in Figure 10, the rotating pair connections at pin 1-4 were replaced by the pin clearance contact model, thus a dynamic model of the multi-clearance coupling support was built. As shown in Table 6, pin 1-4 were selected as four different experimental factors, and the clearance size of 1mm, 2mm and 3mm were selected as three groups of horizontal variables, thus forming the four-factor and

three-level orthogonal test group.

Table. 6. Orthogonal test table.

Test number	Clearance size			
	Pin 1	Pin 2	Pin 3	Pin 4
1	1	1	1	1
2	1	2	2	2
3	1	3	3	3
4	2	1	2	3
5	2	2	3	1
6	2	3	1	2
7	3	1	3	2
8	3	2	1	3
9	3	3	2	1

4.2. Analysis of bearing capacity of hydraulic support under multi-clearance coupling

Figure 15 shows the change of the transmission force of each bearing point in the condition of multiple clearance s compared with the non-clearance. By observing the figure 15, it can be intuitively seen that the transmission force of each bearing point

under multi-clearance coupling presents a greater degree of increase than that without clearance, in which the transmission force of each bearing point under test 1 changes the least, and the transmission force of each bearing point under test 3 changes the most. From Table 6 of the orthogonal test, it can be observed that the total coupling clearance of test 1 and test 3 corresponds to the minimum clearance of 4mm and the maximum clearance of 10mm respectively. Therefore, under the condition of multi-clearance coupling, the coupling clearance size has a positive influence on the transmission force of each bearing point.

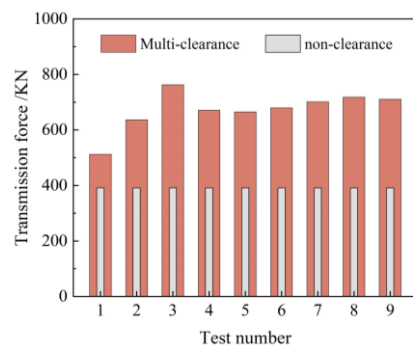
Combined with the data analysis in Table 7, the transmission force of bearing point 3 is 395.7KN when there is no clearance, while the transmission force of test 1 and test 3 is 516.9KN and 767.0KN, respectively, the rate of increase was 30.6% and 93.8% respectively. The transmission force of bearing point 1 without clearance is 391.3KN, while the transmission force of test 1 and test 3 is 512.5KN and 762.6KN, respectively, with an increase ratio of 30.9% and 94.8% respectively.

In addition, according to the static load transmission force of each bearing point with a single clearance size shown in Table 8, combined with the data in Table 7, it can be observed that under the coupling action of multi-clearance, the transmission force of each bearing point is significantly greater than that

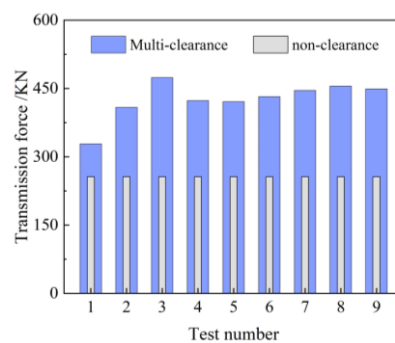
under the action of a single clearance.

Under the action of multi-clearance coupling, the connection attitude between the hydraulic support components will change due to the clearance, which will affect the force transfer direction at the bearing point. According to the transmission force of each bearing point with a single clearance size shown in Table 8, and compared with the data in Table 7, it can be observed that the transmission force of each bearing point is significantly greater than that under the action of a single clearance. When the coupling clearance size is large, the contact force will be generated at a single connection clearance, so that the coupling effect of the clearance will further amplify the impact of the clearance on the transmission force of each bearing point, and the bearing condition of each bearing point will be worse.

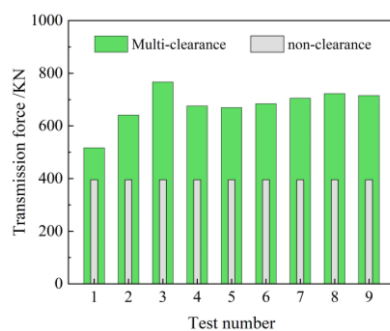
In particular, when the coupling clearance between bearing point 3 and bearing point 1 is 10mm in test 3, the increase of transmission force exceeds 90%, which greatly attenuates the bearing performance of hydraulic support. Therefore, the design of the connection pin at the bearing point 3 and the bearing point 1 should pay attention to, and the hydraulic support should avoid excessive pin clearance in the bearing work to ensure its good bearing performance.



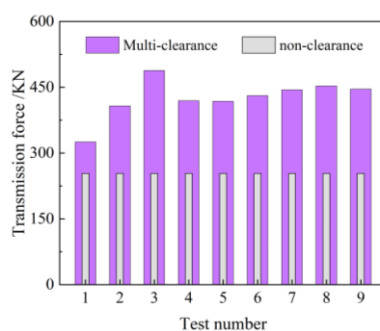
(a) Bearing point 1 transmission force



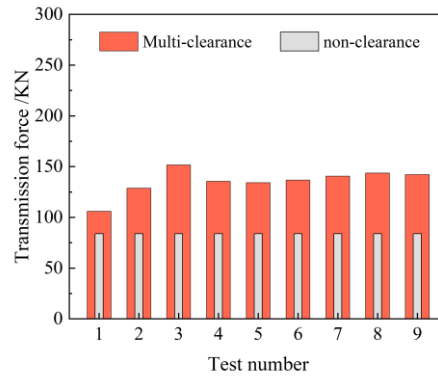
(b) Bearing point 2 transmission force



(c) Bearing point 3 transmission force



(d) Bearing point 4 transmission force



(e) Bearing point 5 transmission force

Fig. 15. Transmission force at the bearing point with multi-clearance and non-clearance.

Table.7. Transmission force of bearing point under multi-clearance coupling.

Test number	Transmit force of bearing point /KN				
	Point 1	Point 2	Point 3	Point 4	Point 5
1	512.5	328.3	516.9	325.3	106.0
2	636.9	408.6	641.4	407.6	128.8
3	762.6	471.1	767.0	488.1	151.6
4	671.4	423.5	675.8	419.3	135.5
5	665.1	421.2	669.5	418.1	134.2
6	679.8	432.3	684.3	430.8	136.8
7	701.0	445.8	705.3	444.1	140.6
8	718.3	455.2	722.8	453.0	143.7
9	711.1	449.1	715.6	446.0	142.2

Table.8. Transmission force of bearing point with single clearance.

Position	Size	Transmit force of bearing point /KN				
		Point 1	Point 2	Point 3	Point 4	Point 5
Pin 1	1mm	417.0	272.0	421.4	269.4	88.5
	2mm	453.5	294.3	457.9	291.7	95.3
	3mm	489.9	316.5	494.3	313.9	101.9
Pin 2	1mm	425.4	276.9	429.8	274.3	90.1
	2mm	469.6	303.6	474.0	301.0	98.1
	3mm	513.6	330.1	518.0	327.5	106.2
Pin 3	1mm	416.2	271.1	420.6	268.5	88.4
	2mm	451.6	293.3	456.0	290.7	94.9
	3mm	488.0	315.8	492.4	313.2	101.6
Pin 4	1mm	425.9	277.0	430.3	274.4	90.1
	2mm	467.6	302.4	472.1	299.8	97.8
	3mm	511.8	329.6	517.0	327	105.4

5. Conclusion

In this paper, the simulation model of hydraulic support without pin clearance was built by means of equivalent column with constant stiffness spring damping system. On this basis, the simulation model of the single-pin clearance and multi-clearance hydraulic support was built. Moreover, the effect of the single-pin clearance and multi-clearance coupling on the

bearing capacity of the hydraulic support was studied. The main results are as following:

- 1) The presence of pin clearance will lead to the increase of the transmission force at the bearing point of the hydraulic support, thus reducing the bearing performance of the hydraulic support, and the larger the clearance size, the more obvious the weakening of the bearing performance of the hydraulic support.
- 2) Among the four single-clearance positions, the front

connecting rod - base pin position has the largest weakening effect on the bearing performance of the hydraulic support, while the rear connecting rod - shield beam pin position has the least weakening effect on the bearing performance of the hydraulic support.

3) The bearing point at both ends of the rear connecting rod has the highest sensitivity to the change of clearance, followed by the bearing point at both ends of the front connecting rod, and the bearing point at the top beam - cover beam is the smallest.

4) Under the condition of multi-clearance coupling, the minimum increase of transmission force at the bearing point is more than 26.3%. Therefore, the coupling effect of the clearance

will further amplify the impact of the clearance on the bearing capacity of the hydraulic support, and seriously threaten the support safety.

To sum up, the existence of the pin connection clearance will weaken the bearing performance of the hydraulic support. Therefore, the connection strength of both ends of the rear connecting rod of the hydraulic support should be appropriately increased, and the clearance size between the key bearing connecting parts should be more critical. Moreover, the clearance of the pin connection is a significant element that cannot be ignored to affect the bearing capacity of the hydraulic support, so it is awfully sense for the development of support devices to further study the hydraulic support with clearance.

Acknowledgement

This work was supported by National Natural Science Foundation of China (Grant No. 52304143, 51974170) and National Natural Science Foundation of Shandong Province (Grant No. ZR2022QE022).

References

1. Ambrósio JAC. Impact of rigid and flexible multibody systems: deformation description and contact models. *Virtual nonlinear multibody systems*, 2003: 57-81. https://doi.org/10.1007/978-94-010-0203-5_4.
2. Bhalerao K, Issac KK. Simulation of impact, based on an approach to detect interference. *Advances in engineering software*, 2006, 37(12): 805-813. <https://doi.org/10.1016/j.advengsoft.2006.05.001>.
3. Brake M R. An analytical elastic-perfectly plastic contact model. *International Journal of Solids and Structures*, 2012, 49(22): 3129-3141. <https://doi.org/10.1016/j.ijsolstr.2015.02.018>.
4. Brake M R W. An analytical elastic plastic contact model with strain hardening and frictional effects for normal and oblique impacts[J]. *International Journal of Solids and Structures*, 2015, 62: 104-123. <https://doi.org/10.1016/j.ijsolstr.2012.06.013>.
5. Bu Q, Tu M, Zhang X, et al. Analysis on energy accumulation-dispersion evolution of thick hard roof and dynamic load response of hydraulic support in large space stope. *Frontiers in Earth Science*, 2022: 572. <https://doi.org/10.3389/feart.2022.884361>.
6. Cao L, Jin X, Qin J, et al. Research on the hydraulic support top beam based on dynamic load bearing. *Frontiers in Earth Science*, 2023, 11: 1171342. <https://doi.org/10.3389/feart.2023.1171342>.
7. Cifuentes A O. Using MSC/NASTRAN: statics and dynamics. Springer Science & Business Media, 2012. <https://doi.org/10.1007/978-1-4613-8917-0>.
8. Flores P, Ambrósio J, Claro J C P, et al. A study on dynamics of mechanical systems including joints with clearance and lubrication. *Mechanism and Machine Theory*, 2006, 41(3): 247-261. <https://doi.org/10.1016/j.mechmachtheory.2005.10.002>.
9. Ge X, Xie J, Wang X, et al. A virtual adjustment method and experimental study of the support attitude of hydraulic support groups in propulsion state. *Measurement*, 2020, 158: 107743. <https://doi.org/10.1016/j.measurement.2020.107743>.
10. Guan E, Miao H, Li P, et al. Dynamic model analysis of hydraulic support[J]. *Advances in Mechanical Engineering*, 2019, 11(1): 1687814018820143. <https://doi.org/10.1177/1687814018820143>.
11. Hertz H. Ueber die Berührung fester elastischer Körper. *Journal reine und angewandte Mathematik*, 1882, (92):156-171. <https://doi.org/10.1515/9783112342404-004>.
12. Hu X, Liu X, Stability analysis of four-column hydraulic support. *Journal of Vibration and Shock*, 2021, 40(19): 1-11+25. <https://doi.org/10.13465/j.cnki.jvs.2021.19.001>.
13. Lankarani H M, Nikravesh P E. Continuous contact force models for impact analysis in multibody systems. *Nonlinear Dynamics*, 1994, 5: 193-207. <https://doi.org/10.1007/bf00045676>.

14. Lankarani HM, Nikravesh PE. A contact force model with hysteresis damping for impact analysis of multibody system//International Design Engineering Technical Conferences and Computers and Information in Engineering Conference. American Society of Mechanical Engineers, 1989, 3691: 45-51. <https://doi.org/10.1115/detc1989-0104>.
15. Li H, Jiang D, Syd S Peng, et al. Analysis on loading features and suitability of hydraulic powered caving supports. *Coal Science & Technology* (0253-2336), 2015, 43(6). <https://doi.org/10.13199/j.cnki.cst.2015.06.005>.
16. Meng Z, Ma C, Xie Y. Influence of impact load form on dynamic response of chock-shield support. *Eksploatacja i Niezawodność – Maintenance and Reliability*. 2023;25(3). <https://doi.org/10.17531/ein/168316>.
17. Pan L, Tang P, Zhou M, et al. Research on prevention and control of rock burst in entry with suspended roof structure [J]. *Coal Science and Technology*, 2022, 50(4): 42-48. <https://doi.org/10.13199/j.cnki.cst.2020-1267>.
18. Pang Y, Liu X, Wang H, et al. Support attitude and height analysis method of hydraulic support based on jack stroke drive. *Journal of Mining & Safety Engineering*, 2023:1-14. <http://kns.cnki.net/kcms/detail/32.1760.TD.20230309.1621.002.html>.
19. Ravn P. A continuous analysis method for planar multibody systems with joint clearance[J]. *Multibody System Dynamics*, 1998, 2:1-24. <https://doi.org/10.1023/A:1009759826529>.
20. Ren H, Zhang D, Gong S, et al. Dynamic impact experiment and response characteristics analysis for 1: 2 reduced-scale model of hydraulic support[J]. *International Journal of Mining Science and Technology*, 2021, 31(3): 347-356. <https://doi.org/10.1016/j.ijmst.2021.03.004>.
21. Tian Z, Jing S, Gao S, et al. Establishment and simulation of dynamic model of backfilling hydraulic support with six pillars. *Journal of Vibroengineering*, 2020, 22(3): 486-497. <https://doi.org/10.21595/jve.2019.20512>.
22. Wan L, Liu P, Meng Z, et al. Study and analysis on stability of hydraulic powered support for ultra-high mining. *Coal Science and technology*, 2017, 45(1):148-153. <http://doi.org/10.13199/j.cnki.cst.2017.01.025>.
23. Wan L, Yu X, Zeng X, et al. Capacity analysis of the new balance jack of anti-impact ground pressure hydraulic support. *Alexandria Engineering Journal*, 2023, 62: 157-167. <https://doi.org/10.1016/j.aej.2022.07.002>.
24. Wang B, Xie J, Wang X, et al. A new method for measuring the attitude and straightness of hydraulic support groups based on point clouds. *Arabian Journal for Science and Engineering*, 2021, 46(12): 11739-11757. <https://doi.org/10.1007/s13369-021-05689-2>.
25. Wang G, Zhang L, Li S, et al. Progresses in theory and technological development of unmanned smart mining system. *Journal of China Coal Society*, 2023, 48(1): 34-53. <http://doi.org/10.13225/j.cnki.jccs.2022.1536>.
26. Wang G. New technological progress of coal mine intelligence and its problems. *Coal Science and technology*, 2022, 50(1): 1-27. <https://doi.org/10.13199/j.cnki.cst.2022.01.001>.
27. Wang G. Study and practice on technical system of hydraulic powered supports. *Journal of China Coal Society*, 2010, 35(11): 1903-1908. <https://doi.org/10.13199/j.cnki.cst.2017.01.025>.
28. Wang S, Li X, Qin Q. Study on surrounding rock control and support stability of Ultra-large height mining face. *Energies*, 2022, 15(18): 6811. <https://doi.org/10.3390/en15186811>.
29. Wang X, Cui T, Xie J, et al. Virtual simulation method of hydraulic support motion considering pin shaft clearance. *Coal Science and technology*, 2021, 49(2): 186-193. <https://doi.org/10.13199/j.cnki.cst.2021.02.022>.
30. Wang X, Yang Z, Feng J, et al. Stress analysis and stability analysis on doubly-telescopic prop of hydraulic support. *Engineering Failure Analysis*, 2013, 32: 274-282. <https://doi.org/10.1016/j.engfailanal.2013.04.006>.
31. Yan S, Xu G, Fan Z, et al. Development course and prospect of the 50 years' comprehensive mechanized coal mining in China. *Coal Science & Technology* (0253-2336), 2021, 49(11). <https://doi.org/10.13199/j.cnki.cst.2021.11.001>.
32. Zeng Q, Li Y, Yang Y. Dynamic Analysis of Hydraulic Support with Single Clearance[J]. *Strojnicki Vestnik/Journal of Mechanical Engineering*, 2021, 67. <https://doi.org/10.5545/sv-jme.2020.6998>.
33. Zeng Q, Xu P, Meng Z, et al. Dynamic response characteristics analysis of four chock shield support under impact load. *Coal Science and Technology*, 2023, 51(1): 437-445. <https://doi.org/10.13199/j.cnki.cst.2022-0975>.
34. Zeng Q, Xu W, Gao K. Measurement Method and Experiment of Hydraulic Support Group Attitude and Straightness Based on Binocular Vision. *IEEE Transactions on Instrumentation and Measurement*, 2023. <https://doi.org/10.1109/TIM.2023.3267344>.
35. Zhang Y, Zhang H, Gao K, et al. New method and experiment for detecting relative position and posture of the hydraulic support. *Ieee Access*, 2019, 7: 181842-181854. <http://doi.org/10.1109/ACCESS.2019.2958981>.